Quantum theory of soliton propagation in an optical fiber using the Hartree approximation

Ewan M. Wright*
Optical Sciences Center, University of Arizona, Tucson, Arizona 87721

(Received 29 October 1990)

The quantum theory of pulse propagation in a nonlinear optical fiber is presented using the time-dependent Hartree approximation. This formulation clarifies the connections between the quantum theory of soliton propagation and single-mode theories that have been used to describe the effects of self-phase modulation. An approximate solution is obtained for coherent-state soliton pulses that gives excellent agreement with numerical calculations for the quadrature phase amplitudes of the field. These amplitudes are found to undergo a series of collapses and revivals with propagation; the first collapse is related to the appearance of interference fringes in the field Q function.

I. INTRODUCTION

It is well known that the combined effects of group velocity dispersion (GVD) and self-phase modulation (SPM) can lead to the formation of temporal optical solitons in optical fibers.[1,2] Classically the propagation of temporal solitons can be described using the nonlinear Schrödinger equation (NLSE). More recently the quantum NLSE has been studied as a model for investigating quantum effects in pulse propagation in nonlinear optical fibers.[3-10] In particular, optical fibers have been used to generate squeezed states of light,[11,12] and to perform quantum nondemolition measurements.[7,13] Tanas and Kielich[14] and Kitagawa and Yamamoto[15] have shown that upon propagating through a nonlinear medium a monochromatic field can become self-squeezed due to SPM. Milburn[16] and Milburn and Holmes[17] have investigated quantum effects due to SPM using an anharmonic oscillator model, and Yurke and Stoler[18] have suggested that this can be used to generate superpositions of macroscopically distinguishable states. In addition, Kennedy and Drummond[19] and Blow *et al.*[20] have developed exact theories which describe the quantum-statistical properties of traveling waves including the effects of SPM.

Early work on solving the quantum NLSE as a model for pulse propagation in nonlinear optical fibers relied on linearizing the nonlinear operator equations obtained in the Heisenberg picture,[3-6] which limits the validity of the results. More recently, based on earlier work by Kaup,[21] Haus *et al.*[7] have employed the inverse-scattering method[22] in their treatment of the quantization of optical solitons, and Yurke and Potasek have solved the initial value problem for the quantum NLSE using a formalism developed by Gutkin.[8] In a pair of recent papers Lai and Haus have developed an approximate quantum theory of solitons in optical fibers, based on the time-dependent Hartree approximation,[23] and an exact solution using Bethe's ansatz.[9,10]

In this paper I investigate the quantum theory of soliton propagation in a nonlinear optical fiber using the time-dependent Hartree approximation. This formulation clarifies the connections between the quantum theory of soliton propagation and single-mode theories that have been used to describe the effects of self-phase modulation.[14,15,24] The development of the theory follows that of Lai and Haus.[9] However, these authors concentrated primarily on finding a *quantum soliton* solution of the problem.[9,10] Here I consider the case of a pulse whose initial profile is the classical soliton solution, which corresponds more closely to the classical version of the problem.[1,2] An approximate solution is obtained for coherent-state soliton pulses which gives excellent agreement with numerical calculations for the quadrature phase amplitudes of the field. These amplitudes are found to undergo a series of collapses and revivals with propagation, the first collapse being related to the appearance of interference fringes in the field Q function.[16,17]

The remainder of this paper is organized as follows. Section II describes the classical and quantum theories of pulse propagation in a nonlinear optical fiber, and introduces the time-dependent Hartree approximation. Numerical results for a coherent-state soliton pulse are presented in Sec. III B along with an approximate analytic solution of the problem in Sec. III C. Collapses and revivals in the field amplitudes and their relation to the field Q function are discussed in Secs. III D and E. Finally, Sec. IV gives the summary and conclusions.

II. CLASSICAL AND QUANTUM PROPAGATION THEORIES

In this section the quantum theory of propagation in a nonlinear optical fiber is described. This discussion closely follows that given by Lai and Haus,[9] and is included both for completeness and to clarify the notation used. First, Sec. II A describes the underlying classical theory and the quantum theory is taken up in Sec. II B. The time-dependent Hartree approximation is then introduced in Sec. II C.

A. Classical theory

The classical problem to be addressed is the propagation of a quasimonochromatic pulse with mean frequency ω in a single-mode, polarization preserving optical fiber. Then assuming that the field may be treated as polarized orthogonal to the direction of propagation (transverse electric field), the electric field may be written in the form

$$\mathbf{E}(\mathbf{r},t)=\mathbf{e}\{u(r)\mathcal{E}(z,t)\exp[i(kz-\omega t)]+\text{c.c.}\}\ , \tag{1}$$

where $\mathbf{e}$ is the unit polarization vector, r and z are the radial (transverse) and longitudinal coordinates, $\mathcal{E}(z,t)$ is the slowly varying electric field envelope, and $u(r)$ is the dimensionless transverse beam profile of the linear guided wave of the single-mode optical fiber which obeys

$$\left[\frac{d^2}{dr^2}+\frac{1}{r}\frac{d}{dr}+\left[\frac{\omega}{c}\right]^2 n^2(r,\omega)\right]u(r)=k^2(\omega)u(r)\ . \tag{2}$$

Here $n(r,\omega)$ describes the linear refractive-index profile of the optical fiber, and $k(\omega)$ is the modulus of the wave vector for the guided wave that can be written in terms of the effective dielectric constant $\epsilon(\omega)$ as

$$k^2(\omega)=\frac{\epsilon^2(\omega)\omega^2}{\epsilon_0 c^2}\ . \tag{3}$$

Using these definitions, and in the usual quasimonochromatic and paraxial approximations, the following propagation equation is easily obtained for the electric field envelope $\mathcal{E}$ including both GVD and the Kerr nonlinearity of the fiber:[25]

$$i\left[\frac{\partial}{\partial z}+\frac{1}{v_g}\frac{\partial}{\partial t}\right]\mathcal{E}=\frac{k_2}{2}\frac{\partial^2\mathcal{E}}{\partial t^2}-\left[\frac{\omega}{c}\right]\Gamma n_2|\mathcal{E}|^2\mathcal{E}\ , \tag{4}$$

where $v_g=(\partial k/\partial\omega)^{-1}$ is the group velocity, $k_2=\partial^2 k/\partial\omega^2$, n_2 is the nonlinear Kerr coefficient of the fiber, and Γ is a geometrical factor given by

$$\Gamma=\frac{\int_0^\infty 2\pi r\ dr|u(r)|^4}{\int_0^\infty 2\pi r\ dr|u(r)|^2}\ . \tag{5}$$

Here it is assumed that $u(0)=1$, and $\mathcal{E}(z,t)$ is therefore the peak electric field in the fiber. In Eq. (4) the first term on the right-hand side describes the effects of GVD, and the second term accounts for the Kerr nonlinearity. Here it is assumed that propagation losses may be neglected and that the fiber may be treated as a transparent nonlinear dielectric medium. It is then straightforward to show that the cycle-averaged energy of the optical field, which is a conserved quantity, is given by[26,27]

$$U=\frac{2\epsilon(\omega)\omega}{v_g k}\int_0^\infty 2\pi r\ dr|u(r)|^2\int dz|\mathcal{E}(z,t)|^2\ . \tag{6}$$

In this paper the specific case of anomalous dispersion $k_2<0$, and positive noninearity $n_2>0$, will be considered, as this is known to give rise to temporal soliton solutions.[1,2]

To proceed the following dimensionless variables are introduced:

$$x=(z-v_g t)/v_g\tau\ ,\quad t'=|k_2|z/2\tau^2=z/L\ , \tag{7}$$

and

$$\mathcal{E}=\left[\frac{\hbar v_g k}{2\epsilon(\omega)V}\right]^{1/2}\phi\ ,\quad \mathcal{E}^*=\left[\frac{\hbar v_g k}{2\epsilon(\omega)V}\right]^{1/2}\phi^\dagger\ . \tag{8}$$

Here $\tau_p=1.76\tau$ is the full width at half maximum of the pulse,[1,2]

$$V=v_g\tau\int_0^\infty 2\pi r\ dr|u(r)|^2 \tag{9}$$

is the effective volume of the pulse, L is the characteristic length over which a pulse of length τ_p would double in width due to GVD alone, and the *electric field per photon* is defined as

$$\mathcal{E}_p=\left[\frac{\hbar v_g k}{2\epsilon(\omega)V}\right]^{1/2}\ . \tag{10}$$

With these definitions, and replacing t' by t for simplicity in notation, Eqs. (4) and (6) become

$$i\frac{\partial\phi}{\partial t}=-\frac{\partial^2\phi}{\partial x^2}-2C\phi^\dagger\phi\phi \tag{11}$$

and

$$U=\hbar\omega\int dx\,\phi^\dagger(x,t)\phi(x,t)\ , \tag{12}$$

where

$$2C=\left[\frac{\omega}{c}\right]\Gamma n_2\mathcal{E}_p^2 L \tag{13}$$

is the *nonlinear phase shift per photon* over the characteristic length L. Note that in the propagation equation (11) the variable $t=z/L$ plays the role of the longitudinal or propagation coordinate, whereas the variable x describes the temporal envelope of the pulse as viewed in a reference frame moving at the group velocity v_g [see Eq. (7)]. Also, even though $\hbar$ has been introduced in Eqs. (8), (10), and (12), the theory is still classical at this stage.

It is easy to verify that the classical NLSE (11) can be obtained from the following Lagrangian density by evaluating the Euler-Lagrange equations of motion:[28]

$$\mathcal{L}=i\hbar\phi^\dagger\frac{\partial\phi}{\partial t}-\hbar\left[\frac{\partial\phi^\dagger}{\partial x}\frac{\partial\phi}{\partial x}-C\phi^\dagger\phi^\dagger\phi\phi\right]\ . \tag{14}$$

Then by introducing the momentum canonically conjugate to ϕ, the corresponding Hamiltonian, which is a conserved quantity, is found to be

$$H=\hbar\int_{-\infty}^{\infty}dx\left[\frac{\partial\phi^\dagger}{\partial x}\frac{\partial\phi}{\partial x}-C\phi^\dagger\phi^\dagger\phi\phi\right]\ . \tag{15}$$

B. Quantum theory

To obtain the quantum version of the classical field theory described by Eq. (11), the Schrödinger picture shall be used. Then to quantize the classical theory the c-number fields $\phi(x,t)$ and $\phi^\dagger(x,t)$ are replaced by the time-independent field operators $\hat{\phi}(x)$ and $\hat{\phi}^\dagger(x)$ which obey the boson commutation relations[28]

$$\begin{gathered}[\hat{\phi}(x),\hat{\phi}^\dagger(x')]=\delta(x-x')\ ,\\ [\hat{\phi}(x),\hat{\phi}(x')]=[\hat{\phi}^\dagger(x),\hat{\phi}^\dagger(x')]=0\ .\end{gathered} \tag{16}$$

The evolution of the field state vector $|\psi(t)\rangle$ is then governed by the Schrödinger equation

$$i\hbar\frac{\partial}{\partial t}|\psi(t)\rangle=\hat{H}_s|\psi(t)\rangle\ , \tag{17}$$

where the second quantized Hamiltonian operator is obtained by replacing the c-number fields by field operators in Eq. (15),

$$\hat{H}_s=\hbar\int dx\left[\frac{\partial\hat{\phi}^\dagger(x)}{\partial x}\frac{\partial\hat{\phi}(x)}{\partial x}-C\hat{\phi}^\dagger(x)\hat{\phi}^\dagger(x)\hat{\phi}(x)\hat{\phi}(x)\right]\ , \tag{18}$$

and normal ordering of the field operators has been adopted.[29]

C. Time-dependent Hartree approximation

In general, the state vector can be expanded in the boson Fock space as[30]

$$|\psi(t)\rangle=\sum_n a_n|\psi_n(t)\rangle\ , \tag{19}$$

where the n-particle state vector is given by

$$|\psi_n(t)\rangle=\frac{1}{\sqrt{n!}}\int dx_1\cdots\int dx_n f_n(x_n,\ldots,x_n,t)\times\hat{\phi}^\dagger(x_1)\cdots\hat{\phi}^\dagger(x_n)|0\rangle\ , \tag{20}$$

$|0\rangle$ being the vacuum state, and the n-particle wave function f_n has the normalization

$$\int dx_1\cdots\int dx_n|f_n(x_1,\ldots,x_n,t)|^2=1\ . \tag{21}$$

The complex coefficients a_n determine the photon statistics of the pulse as $p_n=|a_n|^2$, where p_n is the probability of there being n photons in the field. By substituting Eq. (20) into (17) it can be shown that f_n obeys an equation of motion which is the Schrödinger equation for a one-dimensional system of bosons with δ-function interaction.[9,23] An approximate Hartree wave function is now introduced following Lai and Haus:[9]

$$f_n^{(H)}(x_1,\ldots,x_n,t)=\prod_{j=1}^{n}\Phi_n(x_j,t)\ , \tag{22}$$

where Φ_n has the normalization

$$\int dx|\Phi_n(x,t)|^2=1\ . \tag{23}$$

An equation of motion can be obtained for Φ_n by using the time-dependent Hartree variational method,[23] which yields[9]

$$i\frac{\partial\Phi_n}{\partial t}=-\frac{\partial^2\Phi_n}{\partial x^2}-2C(n-1)|\Phi_n|^2\Phi_n\ . \tag{24}$$

This equation, which is the usual classical NLSE with C replaced by $C(n-1)$, provides a link between the classical and quantum theories, as shall be discussed later.

Using Eqs. (19) and (22) the Hartree approximation for the state vector can be written as

$$|\psi(t)\rangle_H=\sum_n a_n|\psi_n(t)\rangle_H\ , \tag{25}$$

where

$$|\psi_n(t)\rangle_H=\frac{1}{\sqrt{n!}}\left[\int dx\ \Phi_n(x,t)\hat{\phi}^\dagger(x)\right]^n|0\rangle\ . \tag{26}$$

Basically, in the Hartree approximation all n particles in the n-particle state given by Eq. (26) are assumed to have the same field envelope $\Phi_n(x,t)$. The n-particle state (26) is then simply a generalization of the usual n-particle eigenstate for a single-mode field described by the creation and annihilation operators $a^\dagger$ and a:

$$|\psi_n\rangle=\frac{1}{\sqrt{n!}}(a^\dagger)^n|0\rangle\ . \tag{27}$$

In the single-mode case the creation operator $a^\dagger$ creates photons in a given field configuration which obeys Maxwell's equations and the appropriate boundary conditions, for example, a standing wave electromagnetic mode in a box.[31] By comparison, the operator $\int dx\ \Phi_n(x,t)\hat{\phi}^\dagger(x)$ in Eq. (26) creates photons with electric field envelope $\Phi_n(x,t)$.

Yoon and Negle[23] first introduced the time-dependent Hartree approximation in their study of a one-dimensional system of bosons with δ-function interaction. These authors showed that, for a fixed particle number n, this approximation is exact to leading order in n.[23] In this paper I consider a coherent-state pulse with large mean photon number $\langle n\rangle\gg 1$, which means that only large values of $n\simeq\langle n\rangle$ are relevant in Eq. (25), and the time-dependent Hartree approximation is valid. The approximate state vector given by Eq. (25) shall therefore be used in the remainder of this paper.

Finally, some remarks are in order regarding the quantization procedure used here in which it is the classical field envelope $\mathcal{E}$ (or ϕ) which is quantized. In this way both the quasimonochromatic and paraxial approximations are made at the classical level before quantization.[27] This procedure leads to the creation operator $\hat{\phi}^\dagger(x)$ which would apparently create photons at point x. This notion is contrary to the general result of Newton and Wigner that photons are not localizable particles (they do not possess a position operator).[32] However, a recent work by Deutsch and Garrison,[33] which starts from the exact QED theory, shows explicitly that the photon may be treated as localizable to within regions of space large compared with a cubic wavelength of the light. Therefore, if the electric field envelope varies slowly in space and time compared to the mean wavelength and frequency, respectively, which is precisely when the quasimonochromatic and paraxial approximations are valid, the photon may be treated as localizable with the caveat that its position cannot be determined to within a region smaller than a cubic wavelength. This restriction prohibits the treatment of very short pulses, whose effective volume V is less than a cubic wavelength, using the theory developed here.

III. QUANTUM THEORY OF SOLITON PROPAGATION

In this section the theory described in Sec. II is applied to the propagation of a coherent-state pulse in a nonlinear optical fiber.

A. Preliminaries

Throughout this paper I consider a coherent-state pulse which is described by the Poisson distribution

$$a_n = \left[\frac{\langle n \rangle^n}{n!} \right]^{1/2} \exp(-\langle n \rangle /2) , \tag{28}$$

where $\langle n \rangle$ is the mean photon number

$$\langle n \rangle = \sum_{n=0}^{\infty} n p_n . \tag{29}$$

It is well known that the variance in photon number for such a state is $\sigma = \sqrt{\langle n \rangle}$.[31]

The propagation Eq. (24) is now written in the alternative form

$$i\frac{\partial \Phi_n}{\partial t} = -\frac{\partial^2 \Phi_n}{\partial x^2} - \eta \left[\frac{n-1}{\langle n \rangle - 1} \right] |\Phi_n|^2 \Phi_n , \tag{30}$$

where

$$\eta = \left[\frac{\omega}{c} \right] \Gamma n_2 \mathcal{E}_p^2 (\langle n \rangle - 1) L \tag{31}$$

is the nonlinear phase shift produced by $\langle n \rangle$ photons over the characteristic length L. For the special case $n = \langle n \rangle$, and $\eta = 4$, Eq. (30) has a (classical) soliton solution[22]

$$\Phi(x,t) = \Phi_{\langle n \rangle}(x,t) = \Phi_0(x) \exp(it) , \tag{32}$$

with

$$\Phi_0(x) = 2^{-1/2} \mathrm{sech}(x) , \tag{33}$$

which corresponds to a hyperbolic secant pulse with *soliton period* $t_0 = \pi/4$.[1,2] Note that this solution obeys the normalization condition (23). In the remainder of this paper the value $\eta = 4$ shall be used. In addition, it is assumed that for all values of the photon number n in Eq. (24) the initial condition for the electric field envelope is

$$\Phi_n(x,0) = \Phi_0(x) , \quad n = 0,1,2, \ldots . \tag{34}$$

The initial pulse therefore corresponds to a *coherent state with the classical soliton envelope* $\Phi_0(x)$. In contrast, Lai and Haus considered the case in which $\Phi_n(x,0)$ was different for each photon number n, namely, $\Phi_n(x,t)$ was chosen as the fundamental soliton solution of Eq. (24).[9] For the case considered here the initial field envelope is the classical soliton solution of Eq. (30) only for $n = \langle n \rangle$. Yurke and Potasek have solved the initial value problem for the quantum NLSE using a formalism developed by Gutkin,[8] but it seems impractical to use this method for fields with large mean photon numbers.

B. Numerical solutions

Within the Hartree approximation, the quantum averaged value of the electric field envelope is given by

$$\begin{aligned} \langle \phi(x,t) \rangle &= {}_H\langle \psi(t) | \hat{\phi}(x) | \psi(t) \rangle_H \\ &= \sum_n \sum_m a_n a_m^* \; {}_H\langle \psi_m(t) | \hat{\phi}(x) | \psi_n(t) \rangle_H , \end{aligned} \tag{35}$$

with a similar definition for $\langle \phi^\dagger(x,t) \rangle$. This quantity may be evaluated by using the commutators in Eq. (16) to verify the result

$$\hat{\phi}(x) | \psi_n(t) \rangle_H = \frac{n}{\sqrt{n!}} \Phi_n(x,t) \times \left[\int dx \; \Phi_n(x,t) \hat{\phi}^\dagger(x) \right]^{n-1} |0\rangle . \tag{36}$$

Combining Eqs. (28), (35), and (36) yields

$$\langle \phi(x,t) \rangle = \sqrt{\langle n \rangle} \sum_{n=0}^{\infty} p_n \Phi_{n+1}(x,t) , \tag{37}$$

and in a similar manner

$$\langle \phi^\dagger(x,t) \rangle = \sqrt{\langle n \rangle} \sum_{n=0}^{\infty} p_n \Phi_{n+1}^*(x,t) . \tag{38}$$

Here use has been made of the fact that n-particle state vectors corresponding to different numbers of particles are automatically orthogonal,[30] and it has been assumed that $\int dx \; \Phi_{n-1}^*(x,t) \Phi_n(x,t) \simeq 1$ for all n values of interest. This will be true for a coherent state in the limit of large mean photon number $\langle n \rangle$ since the relevant range of n values is roughly $\langle n \rangle \pm \sqrt{\langle n \rangle}$; the variation in the factor $(n-1)/(\langle n \rangle - 1)$ appearing in Eq. (30) is then $\langle n \rangle^{-1/2}$, which vanishes as $\langle n \rangle \to \infty$. Then by introducing the quadrature phase operators defined by

$$\hat{X}_1(x) = \hat{\phi}(x) + \hat{\phi}^\dagger(x) \tag{39}$$

and

$$\hat{X}_2(x) = [\hat{\phi}(x) - \hat{\phi}^\dagger(x)]/i , \tag{40}$$

the following expressions are obtained for the quantum averaged quadrature phase amplitudes:

$$\langle X_1(x,t) \rangle = 2\sqrt{\langle n \rangle} \sum_{n=0}^{\infty} p_n \mathrm{Re}[\Phi_{n+1}(x,t)] \tag{41}$$

and

$$\langle X_2(x,t) \rangle = 2\sqrt{\langle n \rangle} \sum_{n=0}^{\infty} p_n \mathrm{Im}[\Phi_{n+1}(x,t)] . \tag{42}$$

Numerical solutions for $\langle X_{1,2}(x,t) \rangle$ have been obtained by solving the NLSE's in (30) subject to the initial condition (34) for n values between $\langle n \rangle - 4\sigma$ and $\langle n \rangle + 4\sigma$ using the beam propagation method,[34] and performing the summations in Eqs. (41) an (42). Figure 1(a) shows the calculated evolution of $\langle X_1 \rangle$ evaluated at $x = 0$ for $\langle n \rangle = 100$ (all results are for $\eta = 4$). For the soliton solution given in Eq. (32), the classically predicted time evolution of X_1 is $\cos(t)$ (for any value of x), which oscillates with period 2π In contrast, Fig. 1(a) shows that the quantum prediction for $\langle X_1 \rangle$ undergoes a series of *collapses and revivals,* or recurrences, with propagation (the same phenomenon occurs for $\langle X_2 \rangle$). Such recurrences were previously noted by Milburn[16] in the context of an anharmonic oscillator model which corresponds to SPM without GVD, and are reminiscent of the collapses and revivals in the population inversion predicted by the Jaynes-Cummings model.[35,36] The revivals are true quantum effects as they rely on the granular nature

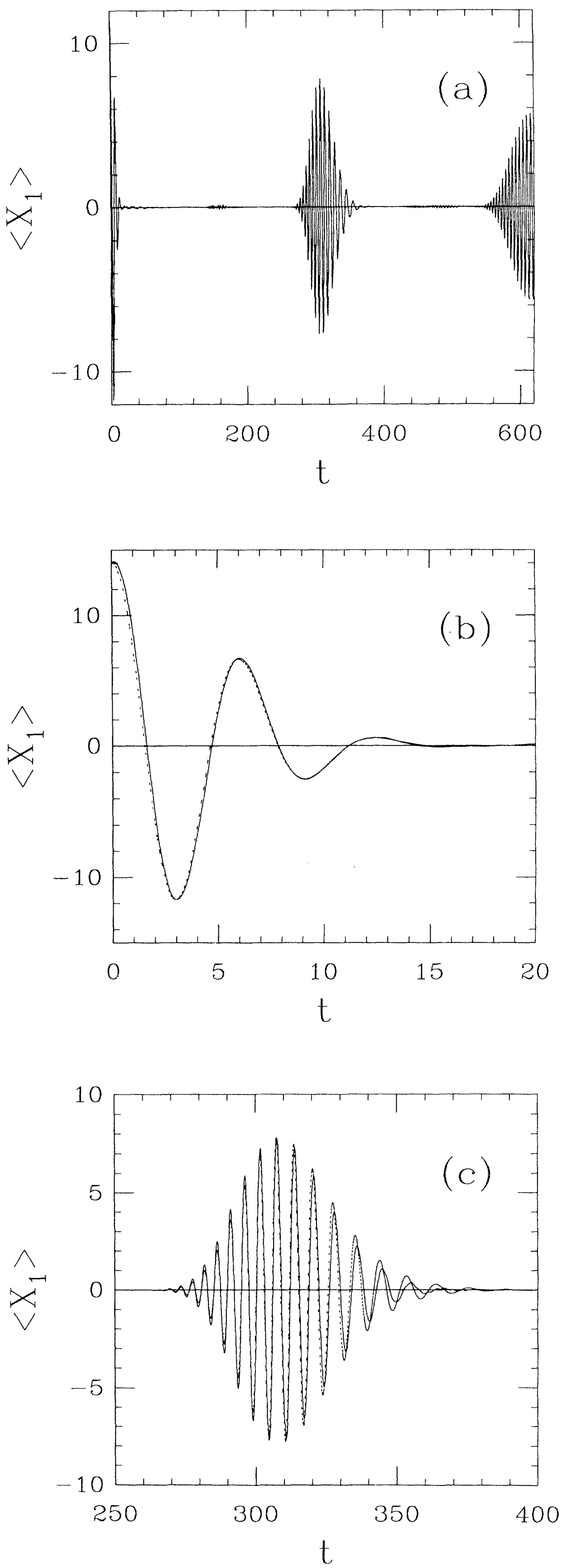

FIG. 1. Quadrature phase amplitude $\langle X_1 \rangle$ vs the dimensionless longitudinal coordinate t for $\langle n \rangle = 100$ and $\eta = 4$. In all plots the numerical solution is shown as the solid line, and in (b) and (c) the approximate solution is shown as a dashed line. Similar results are obtained for $\langle X_2 \rangle$.

of the quantized field as contained in the discrete sums in Eqs. (41) and (42). However, in contrast to the case of pure SPM where the collapses and revivals are perfectly periodic,[16] the collapses and revivals in Fig. 1(a) change with time. The reasons for these similarities and differences shall be taken up in Sec. III D.

The numerical method described here can also be used to calculate a range of quantum averaged quantities, such as the pulse shape and frequency spectrum,[37] and also other photon statistics such as squeezed states.[38]

C. Approximate solution

In order to obtain results for the quadrature phase amplitudes in Eqs. (41) and (42) it is necessary to solve the NLSE (30) subject to the initial condition (34) for each n. This is a large computational job which can take a great deal of CPU time. In this section an approximate solution to the problem is constructed which gives excellent agreement with the numerical results.

In order to construct the approximate solution it is first necessary to review briefly some previous work by Satsuma and Yajima,[39] Doran *et al.*,[40] and Blow *et al.*,[41] on the initial value problem for the classical NLSE. Satsuma and Yajima considered the initial value problem[39]

$$i\frac{\partial u}{\partial t} = -\frac{1}{2}\frac{\partial^2 u}{\partial x^2} - |u|^2 u , \tag{43}$$

with

$$u(x,0) = A \operatorname{sech}(x) . \tag{44}$$

For $A = N$, an integer, one obtains the bound-state multisoliton solutions,[22] $N = 1$ being the fundamental soliton solution which propagates with unchanging intensity profile. For A not an integer the problem can still be solved exactly using the inverse-scattering method,[22] and long-time asymptotic solutions are given in Ref. 39. The remarkable feature of solitons is that they have a uniform value of phase over the whole pulse [see Eq. (32)], but for $A \neq N$ this is no longer strictly true. However, by using the results of Satsuma and Yajima, and through extensive computer simulations, Doran *et al.*[40] and Blow *et al.*[41] have found that for A not too different from 1, the phase of the propagating wave is to a very good approximation homogeneous and given by

$$\begin{aligned} &\theta(t) = 2(A - \tfrac{1}{2})^2 t , \quad A > \tfrac{1}{2} , \\ &\theta(t) = 0 , \quad A < \tfrac{1}{2} . \end{aligned} \tag{45}$$

Furthermore, they show that this phase is directly related to the dominant eigenvalue from the Zakharov-Shabat direct-scattering problem.[22] Here I make the further assumption that A will be close enough to 1 so that any variations in the pulse profile may be neglected. Therefore, if the replacements $t/2 \rightarrow t$, and $u/A\sqrt{2} \rightarrow \Phi$ are made in Eqs. (43)–(44), we obtain the propagation equation

$$i\frac{\partial \Phi}{\partial t} = -\frac{\partial^2 \Phi}{\partial x^2} - 4A^2|\Phi|^2\Phi , \tag{46}$$

with the initial condition

$$\Phi(x,0)=\Phi_0(x)=2^{-1/2}\text{sech}(x)\ , \tag{47}$$

which has the approximate solution

$$\Phi(x,t)\simeq\Phi_0(x)\exp[i\theta(t)]\ . \tag{48}$$

To construct an approximate solution for the quantum problem it is necessary to realize that, for a given photon number n and $\eta=4$, Eq. (46) is identical to Eq. (30) with A^2 playing the role of $(n-1)/(\langle n\rangle-1)$, both propagation equations having the same initial condition [see Eqs. (34) and (47)]. Therefore an approximate solution of Eqs. (30) and (34) for $n \gg 1$ is

$$\Phi_n(x,t)\simeq\Phi_0(x)\exp[i\theta_n(t)]\ , \tag{49}$$

where the photon number dependent phase is given by

$$\theta_n(t)=4\left[\left(\frac{n-1}{\langle n\rangle-1}\right)^{1/2}-\frac{1}{2}\right]^2 t\ , \quad n-1>(\langle n\rangle-1)/4\ , \tag{50}$$

$$\theta_n(t)=0\ ,\quad n-1<(\langle n\rangle-1)/4\ .$$

Then by substituting Eqs. (49) and (50) in (41) and (42) the following approximate expressions are obtained for the quantum averaged quadrature phase amplitudes:

$$\langle X_1(x,t)\rangle=\sqrt{2\langle n\rangle}\ \text{sech}(x)\sum_{n=0}^{\infty}p_n\cos[\theta_{n+1}(t)] \tag{51}$$

and

$$\langle X_2(x,t)\rangle=\sqrt{2\langle n\rangle}\ \text{sech}(x)\sum_{n=0}^{\infty}p_n\sin[\theta_{n+1}(t)]\ . \tag{52}$$

Figures 1(b) and 1(c) show a comparison of the numerically generated results from Sec. II B (solid lines) and the approximate solution (51) (dashed lines) for the evolution of $\langle X_1\rangle$ evaluated at $x=0$, and $\langle n\rangle=100$. Figure 1(b) shows an enlargement of the first collapse shown in Fig. 1(a), and Fig. 1(c) shows the first revival and second collapse. The approximate solution is seen to be in excellent agreement with the full numerical results. This agreement was found to deteriorate quickly for mean photon numbers below $\langle n\rangle=10$.

D. Collapses and revivals

To obtain some insight into the structure of the collapses and revivals in Fig. 1, it is instructive to simplify the photon number dependent phase shift even further. This is done by expanding Eq. (50) in terms of $(n-\langle n\rangle)/\langle n\rangle$, which yields

$$\theta_{n+1}(t)\simeq\left[1+2\left(\frac{n-\langle n\rangle}{\langle n\rangle}\right)+\frac{1}{2}\left(\frac{n-\langle n\rangle}{\langle n\rangle}\right)^2+\cdots\right]t\ . \tag{53}$$

In the limit of a coherent state with large mean photon number $\langle n\rangle\gg 1$, for all n values of interest $(n-\langle n\rangle)/\langle n\rangle$ is of order $\sigma/\langle n\rangle=\langle n\rangle^{-1/2}\ll 1$, and only the first two terms need be retained in Eq. (53) as a first approximation. [Retaining the three terms shown in Eq. (53) is enough to reproduce all the results shown in Fig. 1, whereas the first two terms reproduce only the first collapse precisely.] Then, for example, Eq. (51) becomes

$$\langle X_1(x,t)\rangle\simeq\sqrt{2\langle n\rangle}\ \text{sech}(x)\times\sum_{n=0}^{\infty}p_n\cos\{[1+2(n-\langle n\rangle)/\langle n\rangle]t\}\ . \tag{54}$$

In this approximation the nonlinear phase shift is proportional to the photon number n, which is the case for pure SPM due to a Kerr nonlinearity.[14,15,24] The solution given Eq. (54) predicts collapses and revivals which are perfectly periodic, with a revival period given by

$$t_R=\langle n\rangle\pi\ . \tag{55}$$

This prediction is in excellent agreement with the results in Fig. 1 in which $\langle n\rangle=100$ and the first and second revivals are seen to occur around 100π and 200π, respectively. Recalling that the soliton period t_0 is $\pi/4$, then if z_R and z_0 are the revival and soliton periods in dimensional units

$$z_R=4\langle n\rangle z_0\ . \tag{56}$$

An estimate of the first collapse time can be obtained by replacing the discrete sum in Eq. (54) by a continuum approximation

$$\sum_{n=0}^{\infty}p_n\to\int_0^{\infty}dn\ P(n)\ , \tag{57}$$

where n is treated as a continuous variable in the integral, and using the Gaussian approximation

$$P(n)=\frac{1}{\sqrt{2\pi\langle n\rangle}}\exp[-(n-\langle n\rangle)^2/2\langle n\rangle]\ . \tag{58}$$

Evaluation of the resulting integral yields the simple result

$$\langle X_1(x,t)\rangle\simeq\sqrt{2\langle n\rangle}\ \text{sech}(x)\cos(t)\exp(-2t^2/t_c^2)\ , \tag{59}$$

where the collapse time t_c is given by

$$t_c=\langle n\rangle^{1/2}\ . \tag{60}$$

Therefore, for $\langle n\rangle=100$, $t_c=10$, which is in excellent agreement with the numerical results in Fig. 1(b). In terms of the dimensional collapse length z_c and the soliton period this yields

$$z_c=4z_0\langle n\rangle^{1/2}/\pi\ . \tag{61}$$

Although this simple model for the collapses and revivals provides excellent estimates for the first collapse time and revival period, it cannot explain the fact that the collapses and revivals become broader with time in Fig. 1(a). The reason for the lack of perfect periodicity in Fig. 1 can be traced to the fact that the nonlinear phase shift θ_n in Eq. (50) contains terms proportional to $(n-1)^{1/2}$ as well as $n-1$ due to the combined effects of

GVD and SPM. Weighted sums of trigonometric functions such as those in Eqs. (51) and (52) also appear in the Jaynes-Cummings model, which describes the interaction between a single-mode field and a single two-level atom,[35,36] where the phase is proportional to $t\sqrt{n}$. This model is known to display collapses and revivals in the atomic inversion which appear at regular intervals, but which also broaden with time. Therefore the lack of perfect periodicity in the collapses and revivals in Fig. 1 is due to the fact that we are dealing with soliton propagation which combines GVD and SPM through the phase shift (50), or the three terms shown in Eq. (53), and not simply plane-wave propagation which can be described using SPM alone.[16,18,24] However, the solution given by Eq. (59) for the first collapse is found to agree perfectly with the results shown in Fig. 1 for times short compared to the revival period $t \ll \pi\langle n\rangle$.

Some estimates are useful in order to determine whether the collapses and revivals could be detected in current experiments (although we do not discuss the measurement technique, see, for example, Lai and Haus[42] and Blow *et al.*[43]). For example, Agarwal has shown how the visibility index may be used as a measure of quantum effects resulting from propagation through a nonlinear medium.[24] For concreteness, the parameter values from the optical fiber experiment of Mollenauer *et al.*[2] shall be used while leaving the pulse width τ as a variable parameter. This yields the soliton period as

$$z_0(\mathrm{km}) \simeq 77\times 10^{-3}\tau^2 , \tag{62}$$

and the critical peak power for the fundamental soliton as

$$P_0(W) \simeq (4/\tau)^2 , \tag{63}$$

where τ is in ps. From the critical power the critical pulse energy can be calculated as $U_0 = P_0\tau/2$, and the mean number of photons in the pulse is then found to be ($\lambda = 1.55\ \mu$m)

$$\langle n\rangle = \frac{U_0}{\hbar\omega} \simeq \frac{6.6\times 10^7}{\tau} . \tag{64}$$

Substituting Eqs. (62) and (64) into (56) and (61) then yields

$$z_R(\mathrm{km}) = 4\langle n\rangle z_0 \simeq 10^7\tau \tag{65}$$

and

$$z_c(\mathrm{km}) = 4z_0\langle n\rangle^{1/2}/\pi \simeq 400\tau^{3/2}\ \mathrm{km} , \tag{66}$$

with τ in ps. Taking $\tau = 50$ fs ($\tau_p \simeq 100$ fs) gives $z_c \simeq 10$ km and $z_R \simeq 10^7$ km. It is therefore unrealistic to suggest that even the first revival could be observed in present day (or future) optical fiber experiments, but the collapse length is well within the range of current experiments. (It will, however, be necessary to include the effects of stimulated Raman scattering for such short pulses.[44,45])

As remarked earlier, for times short compared to the revival period, $t \ll \pi\langle n\rangle$, the solution given by Eq. (59) for the first collapse is found to agree precisely with the results shown in Fig. (1). That is, within the experimentally accessible range the photon number dependent phase is well approximated by the first two terms in Eq. (53). This approximation shall be employed in the remainder of this paper.

E. Field Q function

In this section the quasiprobability density (QPD), or Q-function,[46,47] is calculated for an initial coherent state with the classical soliton envelope $\Phi_0(x)$. The QPD is the modulus squared of the projection of the field state vector onto a coherent state, and is a useful means of visualizing different states of an optical field. Lai and Haus have shown that the QPD can be measured using a beamsplitter with two homodyne detectors, and that the quadrature phase amplitudes of the field can be inferred from such measurements.[42] Here the Q function is used to visualize the quantum evolution of the initial soliton.

Consider the following coherent state:

$$|\chi,\alpha\rangle = \exp(-|\alpha|^2 2) \sum_{n=0}^{\infty} \frac{\alpha^n}{\sqrt{n!}}|\chi,n\rangle , \tag{67}$$

where $|\chi,n\rangle$ is an *n-particle eigenstate* with electric field envelope $\chi(x)$,

$$|\chi,n\rangle = \frac{1}{\sqrt{n!}}\left[\int dx\ \chi(x)\hat{\phi}^\dagger(x)\right]^n|0\rangle . \tag{68}$$

By substituting the approximate solution (49) and (50) into the field state vector given by Eqs. (25) and (26) then yields

$$|\psi(t)\rangle_H = \sum_{n=0}^{\infty} a_n \exp[in\theta_n(t)]|\Phi_0,n\rangle , \tag{69}$$

where $\theta_n(t) = [1+2(n-\langle n\rangle)/\langle n\rangle]t$. This approximate field state vector is identical in form to that which appears in the single-mode theory describing SPM alone,[14,15,24] and provides the connection between the two theories. However, what makes the present formulation specific to soliton propagation is the expression for the photon number dependent phase, which combines GVD and SPM, and the classical soliton profile $\Phi_0(x)$ appearing in Eq. (69).

The QPD for the state vector given by Eq. (69) is defined as

$$\begin{aligned} Q_\chi(\alpha,t) &= |\langle \alpha,\chi|\psi(t)\rangle_H|^2 \\ &= \exp[-(|\alpha|^2+\langle n\rangle)] \\ &\quad\times\left|\sum_{n=0}^{\infty}\frac{[\alpha^*\sqrt{\langle n\rangle}(\chi,\Phi_0)]^n}{n!}\exp[in\theta_n(t)]\right|^2 , \end{aligned} \tag{70}$$

where the factor (χ,Φ_0) accounts for the projection of the coherent-state field envelope χ onto the soliton envelope Φ_0. Therefore $Q_\chi(\alpha,t)$ is the probability density at time t for the field to be a coherent state of amplitude α with field envelope $\chi(x)$. For this presentation it is assumed that $\chi = \Phi_0$, $Q_\chi = Q_0$, so that $(\chi,\Phi_0) = 1$.

Kitagawa and Yamamoto[15] employed the Q function to show that upon propagation through a Kerr medium a monochromatic field can become self-squeezed.[14] Lai and Haus have shown that self-squeezing of quantum solitons can occur for propagation lengths less than a soliton period.[9] This means that for a mean photon number $\langle n \rangle \gg 1$, self-squeezing occurs well before the first collapse is complete. Figure 2 shows the evolution of the Q function according to Eq. (70) for $\langle n \rangle = 100$, which is the same as Fig. 1. Here $Q_0(\alpha,t)$ is shown as a function of the real and imaginary parts of α. The initial Q function at $t=0$ is shown in Fig. 2(a), and is a Gaussian centered around $\mathrm{Re}(\alpha)=\sqrt{\langle n \rangle}=10$. Upon propagation the initial soliton becomes self-squeezed as shown in Fig. 2(b) for $t=\frac{1}{2}<t_0$.[15] As the propagation distance is further increased, the self-squeezing effect increases leading to the formation of a "whorl" as shown in Fig. 2(c) for $t=3$.[16,17] However, beyond this point the two ends of the whorl in Fig. 2(c) start to overlap and give rise to interference fringes; this is shown in Fig. 2(d) for a time equal to the collapse time $t_c=10$. Indeed, the first collapse of the quadrature phase amplitude shown in Fig. 1 is connected with the formation of these interference fringes. That is, when the Q function becomes distributed over the full complex-α plane as in Fig. 2(d), the field averaged over the QPD will tend to vanish.[48] In contrast, in Fig. 2(b) the Q function is concentrated mainly in the lower-half complex-α plane and therefore leads to a finite field value upon averaging over the QPD. The formation of the whorl and the interference fringes could potentially be observed in current experiments since they only require fiber lengths of the order of the collapse length.

IV. SUMMARY AND CONCLUSIONS

In this paper the quantum theory of soliton propagation in a nonlinear optical fiber using time-dependent Hartree approximation has been presented. An approximate solution was then developed for coherent-state pulses using the results of Doran *et al.*[40] and Blow *et al.*[41] for the initial value problem for the classical NLSE.[39] This approximate solution, which is given by the field state vector in Eqs. (51) and (52), provides the connection between the quantum theory of soliton propagation and previous single-mode theories based on SPM, in which the photon number dependent phase is proportional to $n-1$.[14,15,24] In contrast, soliton propagation is characterized by the more complex phase shift given in Eq. (50) which contains terms proportional to both $n-1$ and $\sqrt{n-1}$. The validity of the approximate solution was verified by comparison with numerical results for the quadrature phase amplitudes of a coherent-state soliton pulse. These amplitudes were found to undergo a series

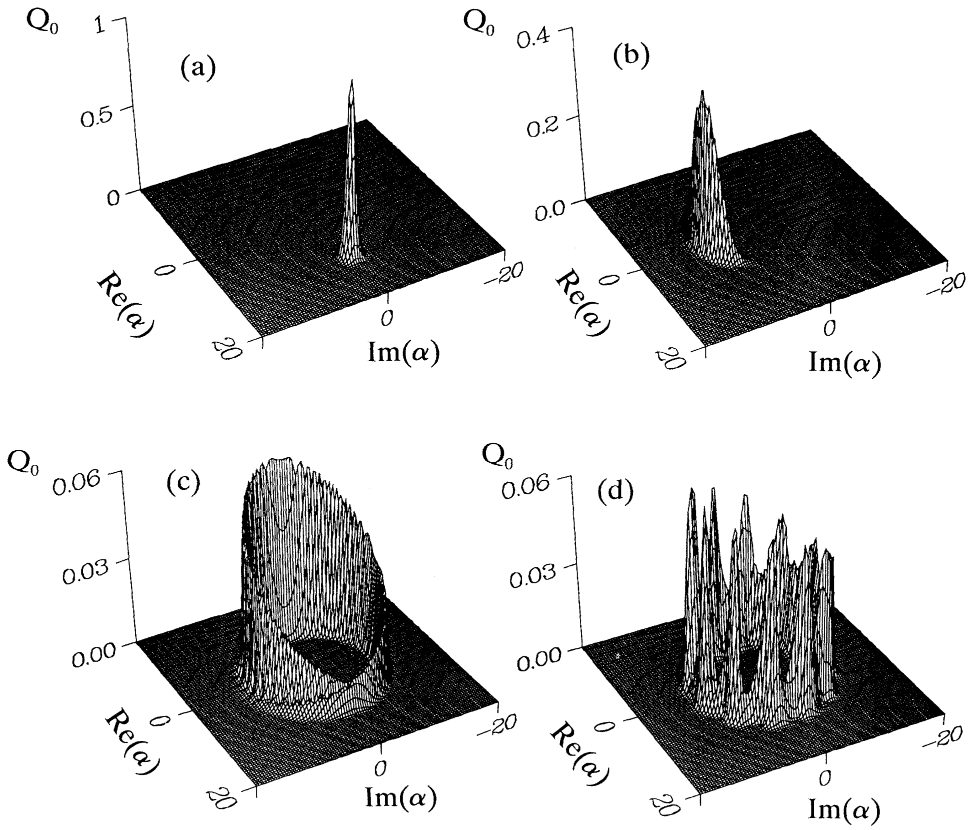

FIG. 2. Grid plot of the QPD $Q_0(\alpha,t)$ vs the real and imaginary parts of α for $\langle n \rangle = 100$ and various values of the dimensionless longitudinal coordinate; (a) $t=0$; (b) $t=\frac{1}{2}$; (c) $t=3$; and (d) $t=t_c=10$.

of collapses and revivals with propagation, and the relation of the first collapse to the appearance of interference fringes in the field Q function was discussed.

In principle, an exact solution for the quantum problem addressed here already exists using the quantum inverse-scattering method,[7,21] without resort to the time-dependent Hartree approximation. This is so because both the classical and quantum NLSE's are integrable systems.[21,22] It will therefore be of great interest to eventually compare the exact solutions with those obtained here. However, the time-dependent Hartree approximation discussed here also allows for the treatment of nonintegrable cases, such as the nonlinear coupled mode problems which occur in birefringent fibers[49] and optical fiber couplers.[50] Such problems cannot in general be solved using the inverse-scattering method and the approach given here should be of great use.

ACKNOWLEDGMENTS

The author would like to thank Dr. Martin Wilkens for his critical reading of the manuscript, and Pierre Meystre and Sophie La Rochelle for several illuminating discussions. This work was supported by the Joint Services Optical Program.

*Also with the Physics Department, University of Arizona, Tucson, AZ 87721.

[1]A. Hasegawa and F. Tappert, Appl. Phys. Lett. **23**, 142 (1973).
[2]L. F. Mollenauer, R. H. Stolen, and J. P. Gordon, Phys. Rev. Lett. **45**, 1095 (1980).
[3]M. J. Potasek and B. Yurke, Phys. Rev. A **35**, 3974 (1987).
[4]M. J. Potasek and B. Yurke, Phys. Rev. A **38**, 1335 (1988).
[5]P. D. Drummond and S. J. Carter, J. Opt. Soc. Am B **4**, 1565 (1987).
[6]S. J. Carter, P. D. Drummond, M. D. Reid, and R. M. Shelby, Phys. Rev. Lett. **58**, 1841 (1987).
[7]H. A. Haus, K. Watanabe, and Y. Yamamoto, J. Opt. Soc. Am B **6**, 1138 (1989).
[8]B. Yurke and M. J. Potasek, J. Opt. Soc. Am B **6**, 1227 (1989).
[9]Y. Lai and H. A. Haus, Phys. Rev. A **40**, 844 (1989).
[10]Y. Lai and H. A. Haus, Phys. Rev. A **40**, 854 (1989).
[11]R. M. Shelby, M. D. Levenson, S. H. Perlmutter, R. G. DeVoe, and D. F. Walls, Phys. Rev. Lett. **57**, 691 (1986).
[12]B. L. Schumaker, S. H. Perlmutter, R. M. Shelby, and M. D. Levenson, Phys. Rev. Lett. **58**, 357 (1987).
[13]M. D. Levenson, R. M. Shelby, M. Reid, and D. F. Walls, Phys. Rev. Lett. **57**, 2473 (1986).
[14]R. Tanas and S. Kielich, Opt. Commun. **45**, 351 (1983).
[15]M. Kitagawa and Y. Yamamoto, Phys. Rev. A **16**, 1451 (1986).
[16]G. J. Milburn, Phys. Rev. A **33**, 674 (1986).
[17]G. J. Milburn and C. A. Holmes, Phys. Rev. Lett. **56**, 2237 (1986).
[18]B. Yurke and D. Stoler, Phys. Rev. Lett. **57**, 13 (1986).
[19]T. A. B. Kennedy and P. D. Drummond, Phys. Rev. A **38**, 1319 (1988).
[20]K. J. Blow, R. Loudon, and S. J. D. Phoenix (unpublished).
[21]D. J. Kaup, J. Math. Phys. **16**, 2036 (1975).
[22]V. E. Zakharov and A. B. Shabat, Zh. Eksp. Teor. Fiz. **61**, 118 (1971) [Sov. Phys.—JETP **34**, 62 (1972)].
[23]B. Yoon and J. W. Negle, Phys. Rev. A **16**, 1451 (1977).
[24]G. S. Agarwal, Opt. Commun. **72**, 253 (1989).
[25]See, for example, G. P. Agarwal, *Nonlinear Fiber Optics* (Academic, Boston, 1989), Chap. 5.
[26]L. D. Landau and E. M. Lifshitz, *Electrodynamics of Continuous Media*, 2nd ed. (Pergamon, Oxford, 1966), p. 275.
[27]T. A. B. Kennedy and E. M. Wright, Phys. Rev. A **38**, 212 (1988).
[28]L. Schiff, *Quantum Mechanics* (Wiley, New York, 1950).
[29]M. Hillery and L. D. Mlodinow, Phys. Rev. A **30**, 1860 (1984).
[30]See, for example, K. Huang, *Statistical Mechanics*, 2nd ed. (Wiley, New York, 1987), Appendix A.
[31]See, for example, P. Meystre and M. S. Sargent III, *Elements of Quantum Optics* (Springer-Verlag, Berlin, 1990).
[32]T. D. Newton and E. P. Wigner, Rev. Mod. Phys. **21**, 400 (1949).
[33]I. H. Deutsch and J. C. Garrison, Phys. Rev. A (to be published).
[34]See, for example, J. A. Fleck, J. R. Morris, and E. S. Bliss, IEEE J. Quantum Electron. **QE-14**, 353 (1978).
[35]E. T. Jaynes and F. W. Cummings, Proc. IEEE **51**, 89 (1963).
[36]J. H. Eberly, N. B. Narozhny, and J. J. Sanchez-Mondragon, Phys. Rev. Lett. **44**, 1323 (1980).
[37]E. M. Wright, J. Opt. Soc. Am. B **7**, 1142 (1990).
[38]D. F. Walls, Nature (London) **306**, 141 (1983).
[39]J. Satsuma and N. Yajima, Prog. Theor. Phys. Suppl. **55**, 284 (1974).
[40]N. J. Doran, K. J. Blow, and D. Wood, Proc. Soc. Photo-Opt. Instrum. Eng. **836**, 238 (1987).
[41]K. Blow, N. J. Doran, and B. K. Nayar, Opt. Lett. **14**, 754 (1989).
[42]Y. Lai and H. A. Haus, Quantum Opt. **1**, 99 (1989).
[43]K. J. Blow, R. Loudon, S. J. D. Phoenix, and T. J. Shepard, Phys. Rev. A **42**, 4102 (1990).
[44]K. J. Blow and D. Wood, IEEE J. Quantum Electron. **QE-25**, 2665 (1989).
[45]R. H. Stolen, J. P. Gordon, W. J. Tomlinson, and H. A. Haus, J. Opt. Soc. Am. B **6**, 1159 (1989).
[46]See, for example, R. J. Glauber, in *Quantum Optics and Electronics*, edited by C. M. DeWitt (Gordon and Breach, New York, 1965).
[47]P. D. Drummond, C. W. Gardiner, and D. F. Walls, Phys. Rev. A **24**, 914 (1981).
[48]For a related discussion in the context of the Jaynes-Cummings model see J. Eiselt and H. Risken, Opt. Commun. **72**, 351 (1989).
[49]C. R. Menyuk, IEEE J. Quantum Electron. **QE-23**, 174 (1987).
[50]S. Trillo, S. Wabnitz, E. M. Wright, and G.I. Stegeman, Opt. Lett. **13**, 672 (1988).